Origami-based metamaterial to attenuate the impact load in a landing gear for the recovery of the Microsatellites Launch Vehicle first stage

Hernani Cordeiro Dionísio[1], Jesús Antonio García Sánchez[1], Luís Antonio Silva[2]

[1]*Institute of Mechanical Engineering, Federal University of Itajubá*
Av. BPS, 1303, Pinheirinho, Itajubá, 37500-903, Minas Gerais, Brazil
hernanicd@unifei.edu.br, jesus@unifei.edu.br
[2]*Prodmec Eletromecânica Ltda*
Rodovia BR 459, Km 124, Chácara Lagoa, Santa Rita do Sapucaí, 37540-000, Minas Gerais, Brazil
engenharia@prodmec.com.br

Abstract. The metamaterials have been studied and pointed as the future of many engineering areas, such as mechanical, aeronautical, civil and electrical. A metamaterial structure differs from another due to the geometry of the unit cell, which provides unique physical properties. Among those properties, it is found the high capacity to absorb and mitigate impact loads. It was verified the viability of applying an origami structure in a landing gear for the Microsatellites Launch Vehicle (VLM-1), the binational project between Brazil and Germany, aiming to recover its first stage. The dynamic response of that structure is compared to a classical structure and the reaction force in the connection between the vehicle and the landing gear is mainly analyzed. The verification was carried out numerically, though impact analysis simulated in the commercial software *ANSYS*®. The results reveal that the studied application is feasible, attenuating the force reaction in the extremities of the leg in contact with the vehicle.

Keywords: Metamaterials, Numerical Analysis, Impact Simulation, Microsatellites Launch Vehicle, Landing Gear.

1 Introduction

Metamaterials (Ms) are man-made structures with counterintuitive mechanical properties that originate in the geometry of their unit cell instead of the properties of each component. These unusual material properties are derived from their microstructural geometry, rather than from their material composition [1].

Metamaterials are, normally, classified according with their physical application, e.g., electromagnetic, optical, thermal, acoustic, mechanical, among others. Impact mitigation properties are characteristics of some metamaterials, which have been studied by many researchers [2]. In this work, we will study one type of Mechanical Metamaterials (MMs), the origami-based mechanical metamaterials (OBMMs).

Deployable structures are typically made of thin membranes and slender elements, which often require foldable, yet stiff, mechanical properties [3]. Originally considered as an ancient art of paper folding, origami has widened its engineering applications significantly in recent decades, being highlighted in several researches around the world [4]. Potential applications of origami-based structures are abundant, including deployable habitats for space exploration and disaster relief, deployable solar arrays and antennas, actively-controlled aerodynamic surfaces, and impact mitigation structures. Therefore, the OBMMs can be pointed as deployable or foldable structures.

A recent study conducted by Yasuda et al. [5] explored the principles underlying the art of origami paper folding applied to design sophisticated MMs with unique mechanical properties and highlighted its potential to be applied in aerospace structures. The designed OBMM structure was capable to form rarefaction solitary waves. The analytical, numerical, and experimental results demonstrated that these rarefaction waves overtake the initial compressive strain waves (caused by the impact loads) in the form of traction strain waves, thereby causing the latter part of the origami structure to feel tensile forces first instead of compression forces under impact. The results

obtained by the authors reveal that the proposed OBMM can be used to create a highly efficient and reusable impact mitigating system without relying on material damping, plasticity or fracture.

Considering that in recent years the aerospace industry has focused on turning rockets into reusable vehicles, then OBMMs structures are a possible feasible solution to attenuate the impact in their landing. In this line, the aerospace company *Space Exploration Technologies Corporation* (SpaceX) introduced a new perspective with the landing of the Falcon 9 rocket first stage in 2017. The achievement was only possible due to the vehicle landing subsystem, composed of support legs, that suffered low-velocity impact loads during the landing phase.

The main objective of this work is to verify the viability of applying OBMMs in a landing gear structure, aiming to recover the first stage of the Microsatellites Launch Vehicle (VLM-1), the binational project between Brazil and Germany, developed by Brazilian Institute of Aeronautics and Space (IAE) and by German DLR – Moraba (*Mobile Raketenbasis*). The VLM-1 project goal is to develop a vehicle composed by three stages, to launch microsatellites in equatorial or re-entry Low Earth Orbits (LEO), as presented by Lacerda [6]. Figure 1 shows this rocket and its principal systems.

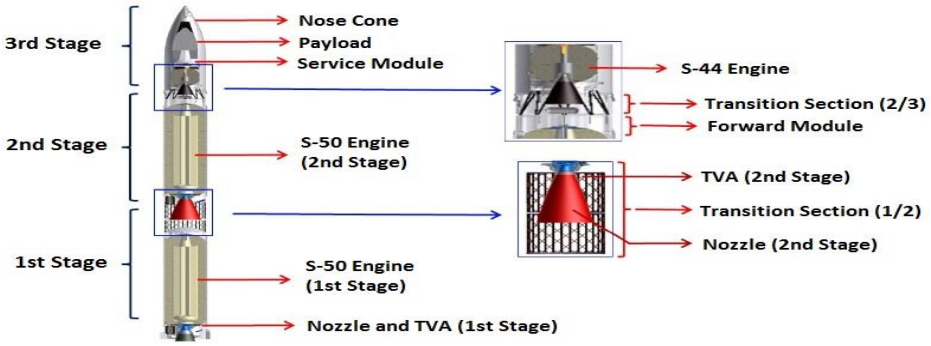

Figure 1. VLM-1 and its principal systems [6]

In summary, we proposed a landing gear structure composed by an OBMM to mitigate the effects of the low-velocity impact loads on VLM-1 during landing. The impact conditions were simulated using the Explicit Dynamics Module of the commercial software *ANSYS*®. To verify the advantages of the proposed structure, its dynamic response is compared with the response of a classical (no MMs) landing gear.

2 Geometries and Materials

2.1 Origami-based metamaterial structure

Figure 2 presents the metamaterial studied and applied in the landing legs that compose the landing gear. This origami-based structure was created in *Autodesk Inventor*® commercial software and its construction was based on the work of Yasuda et al. [5]. It consists of the repetition of an origami cell that is composed by two solids with hexagon shape connected by thin surfaces.

Figure 2. Origami-based metamaterial structure

2.2 First stage, landing gears and landing base projects

The geometry of the first stage is shown in Figure 4. The landing gears were projected according to the dimension values of the first stage of VLM-1, as reported in Table 1.

The aerodynamic influence on the vehicle performance in liftoff was considered in the process of designing

the landing gear structural system. The structural system consists of four landing legs, and its actuation system is composed of two identical rings. The lower ring is fixed, while the upper ring is free to move along the body of the S-50 engine. Considering the pin connections among the legs and the rings, the extension and retraction processes are executed by movement transmission between them, as also shown in Figure 4.

Table 1. VLM-1 first stage geometrical parameters

Parameter	Value
S-50 Engine External Diameter (mm)	1460
First Stage Length (mm)	5400
Fin Length (mm)	800
Nozzle Length (mm)	600
Nozzle External Diameter (mm)	1300

2.3 Reference landing leg

Based on Falcon 9 landing legs and after several impact simulations, the reference landing leg was designed using the dimension values reported in Table 1. It consists of three bars connected by a pin that allows them to rotate. Figure 3 shows the geometry of the reference leg where it is possible to observe the three fixing holes that connect the leg to the rings from the actuation system by pins as well. To differ the landing legs, this one was named L-r-CF due to the Carbon Fiber material employed in the simulations.

L-r-CF main purpose is to serve as a comparison for the origami-based landing leg. Both were designed with the same dimensions and their configuration at the impact moment are equal (the angle between the upper and lower bars of both legs at the impact moment is 20°), for the comparison of the results to be the fairest.

2.4 Origami landing leg

The dimensions used to design the origami landing leg, named L-ori, were identical to those of the L-r-CF. Figure 3 also shows L-ori where it is possible to analyze the similarities and differences between the two legs.

The origami surfaces thickness is 10 mm and their assigned material is Al 2024 T6, parameters that were determined after obtaining better results in the impact simulations. The same Carbon Fiber material employed in L-r-CF was assigned to all other L-ori components.

2.5 Landing base

Figure 3 also demonstrates the landing base used in all impact simulations. Its dimensions were established in a way to allow the landing leg impact to occur on its center, with a clearance for possible slips.

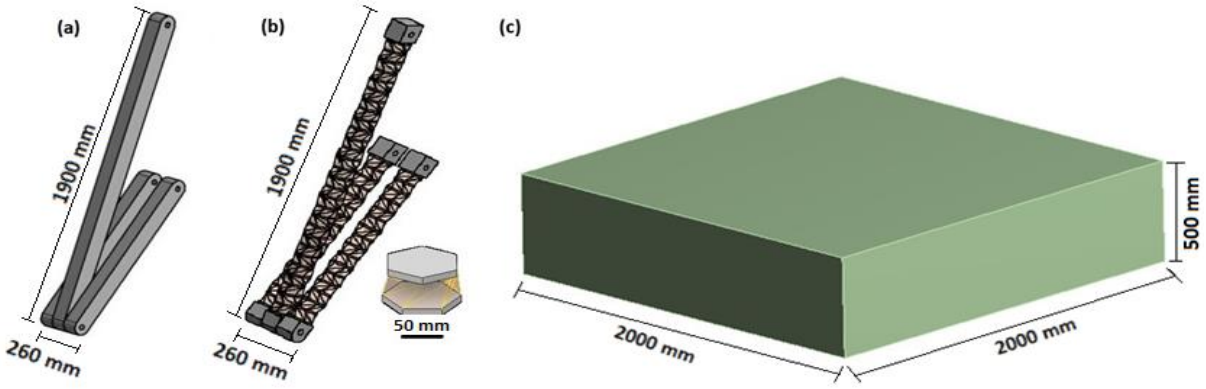

Figure 3. Geometries: (a) L-r-CF, (b) L-ori, (c) Landing base

2.6 Complete assemblies

Figure 4 demonstrates the reference and the origami-based landing gear implemented to the VLM-1 first stage.

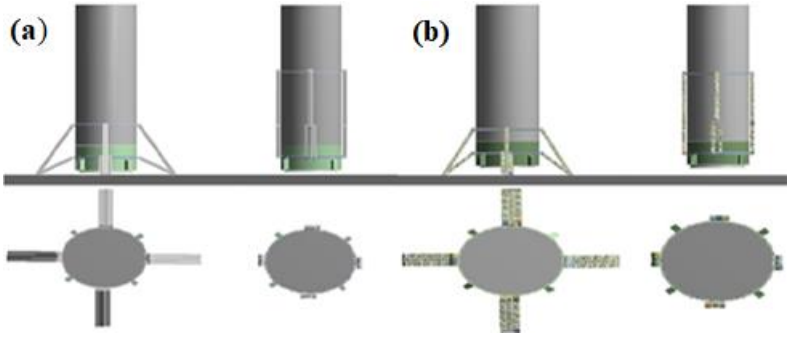

Figure 4. Front and upper views of the landing gears: (a) L-r-CF, (b) L-ori

2.7 Materials

After several impact simulations, better results were obtained when the materials presented in Table 2 were employed in the landing legs. It is important to emphasize that the material "Structural Steel" was employed only in the landing base, to avoid as much impact load absorption by the base, directing it all to the legs.

Table 2. Mechanical properties of the employed materials [7]

Material	Density (kg/m^3)	Young Modulus (GPa)	Tensile Strength (MPa)	σ_y (MPa)	σ_u (MPa)	Poisson Ratio (-)
Structural Steel	7850	200	(-)	250	400	0.3
Carbon Fiber	1800	230	3500	(-)	1500	0.2
Al 2024 T6	2770	73.8	(-)	345	427	0.337

Table 3 reports the mass values of the landing gears and their components. It is important to note that the total masses of the landing gears did not exceed the maximum permitted value of 400 kg. Moreover, the clearances allow the addition of hydraulic and electric components of the actuation system.

Table 3. Mass values of the landing gears and their components

Component	Mass (kg)
L-r-CF landing gear (complete)	274
Origami landing gear (complete)	186
Actuation system (rings)	22
L-r-CF landing leg (unit)	63
L-ori landing leg (unit)	41

3 Boundary Conditions

3.1 Maximum landing velocity

According to O'Connel [8], the first stage of the rocket Falcon 9, developed and produced by *SpaceX*, lands with a landing velocity of approximately 20 km/h, after being decelerated by the central engine propulsion. It was

defined that the landing velocity of the VLM-1 first stage will have the same value, to be applied in the impact simulations which results will be presented.

3.2 Maximum landing weight

According to Lacerda [6], the dry mass of the VLM-1 first stage, that is, considering the engine out of propellant, is approximately 1500 kg. Besides, considering the theoretical S-50 engine thrust in a vacuum of 550 kN and that the payload will be maximum, the mass value of the proposed landing gear subsystem cannot exceed 400 kg, under penalty of over-compromising the mission. It was considered as well 100 kg of residual propellant, which cannot have been burned during the landing phase.

It was determined then the maximum mass value of the VLM-1 first stage at the moment of touch between the landing legs and the landing base, given by the following equation:

$$m_L = m_S + m_T + m_P \tag{1}$$

where m_L is the VLM-1 first stage maximum mass, m_S is the VLM-1 first stage dry mass, m_T is the mass of the landing gear subsystem and m_P is the mass of the residual propellant. The value obtained for m_L was 2000 kg.

The maximum weight of the VLM-1 first stage is expressed by:

$$P_L = m_L g \tag{2}$$

where P_L is the VLM-1 first stage maximum weight and g is the acceleration due to gravity, assumed as 9.81 m/s^2. The value obtained for P_L was 19.62 kN. This value was rounded to 20 kN to ensure greater clearance in the value of weight that the landing gear must bear.

4 Finite Element Modeling of Low-Velocity Impact

4.1 Finite element models

The 3D finite element model is established based on the available data given by Zhou et al [1]. The Explicit Dynamics Module of the commercial software *ANSYS*® was used to execute the dynamic analysis of the reference and the origami landing legs. In order to reduce simulation time and computational cost, it was decided to simulate only one landing leg at a time, considering that the landing is perfectly vertical and that the conditions are the same for all four landing legs of each landing gear. So, it was necessary to divide the maximum weight of the VLM-1 first stage during the landing phase by the number of landing legs which is four. Therefore, the load value applied in the three fixing holes is 5 kN along the z-axis. The distance between the nearest surfaces of the landing leg and the top face of the landing base is set as 10 mm. The initial velocity of 6 m/s along the z-axis is assigned to the landing leg. All freedoms along the x-axis and y-axis are constrained to zero using the *Displacement* support applied to the surfaces of the three fixing holes. The landing base is fixed by applying for the *Fixed* support on its surface as opposed to that faced to the landing leg. The simulation time is set as 0.03 s.

4.2 Element types, mesh density and contact definition

For the L-r-CF model, the element Hex8 is used in the landing base with element size of 5 cm. The elements Hex8 and Wed6 are used in the L-r-CF with element size of 1.5 cm. Therefore, the mesh consists of 27286 Hex8 elements and 420 Wed6 elements.

For the L-ori model, the element Hex8 is used in the landing base with element size of 4 cm. The elements Hex8, Wed6, Tri3 and Quad4 are used in the origami landing leg with element size of 1.5 cm. Therefore, the mesh consists of 17098 Hex8 elements, 1152 Wed6 elements, 2410 Tri3 elements and 5250 Quad4 elements.

The contact mode adopted is *Automatic* and its type is *Bonded*, reducing the computational cost.

5 Numerical Results and Discussion

The results obtained for each landing leg were: Equivalent Stress, Total Deformation, Equivalent Elastic Strain and two Force Reaction x Time graphics, one for the upper fixing hole and one for the under fixing holes.

5.1 L-r-CF and L-ori results

Figures 7 and 8 present the results of Equivalent Stress, Total Deformation and Equivalent Elastic Strain for L-r-CF and L-ori respectively.

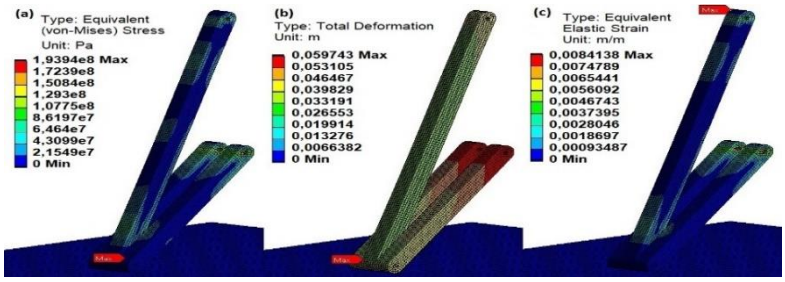

Figure 7. L-r-CF results: (a) equivalent stress, (b) total deformation, (c) equivalent elastic strain

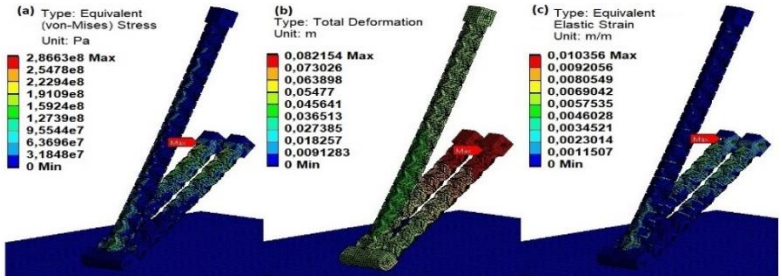

Figure 8. L-ori results: (a) equivalent stress, (b) total deformation, (c) equivalent elastic strain

5.2 Comparison between results

This topic aims to verify which of the landing legs showed the best results. The main measure of comparison was the force reaction in the fixing holes. Figure 9 presents the comparative graphics. Table 4 reports the maximum values of each parameter obtained in the impact simulation for each landing leg. It is possible to observe that the maximum values of equivalent stress are quite smaller than the yield stress of the respective employed materials.

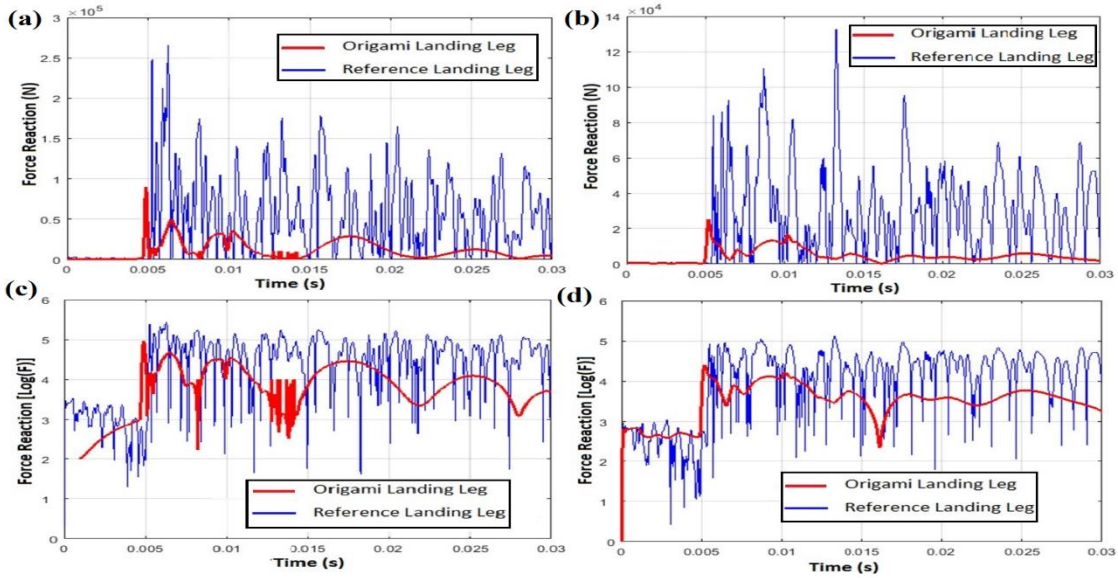

Figure 9. Force reaction x Time comparative graphics: (a) [N] x [s] in the under fixing holes, (b) [N] x [s] in the upper fixing hole, (c) [Log(F)] x [s] in the under fixing holes, (d) [Log(F)] x [s] in the upper fixing hole

Table 4. Maximum values obtained in the impact simulations

Parameter	Value for L-r-CF	Value for L-ori
Equivalent Stress (MPa)	193.94	286.67
Total Deformation (mm)	59.743	82.147
Equivalent Elastic Strain (m/m)	0.0084138	0.010353
Force Reaction in the under fixing holes (kN)	265.76	89.783
Force Reaction in the upper fixing hole (kN)	132.69	25.299

6 Conclusions

Noting that the origami-based landing leg was submitted to the very same boundary conditions assigned to its respective reference landing leg, that the maximum equivalent stresses obtained for both legs are under the respective yield strength of the employed materials, that the dimensions of each leg are practically identical and that the total masses of both landing gears did not exceed the limit of 400 kg, it is concluded that the use of the tested origami-based metamaterial in a landing gear employed in the recovery of the VLM-1 first stage is feasible.

It was found that the implementation of the origami-based metamaterial reduced approximately 66% of the maximum force reaction value in the under fixing holes and approximately 81% of the maximum force reaction value obtained in the upper fixing hole of L-r-CF. Such results indicate that its viable to make use of this application, since, despite the possibly higher manufacturing cost, the significant mitigation of the force reaction due to the impact reveals several advantages listed as follows:

- Decrease in the mass of the first stage with landing gear attached (considering the respective reference landing leg);
- Possible increase of the number of landing legs reducing, even more, the force reaction and rising the stability of the landing phase (considering the previous advantage);
- Possible increase of the maximum landing velocity, reducing the necessary fuel quantity to slow down the first stage;
- Reduction of the failure risk during the landing phase, particularly in the fixing holes, increasing the mission reliability.

Acknowledgements. We thank Major Engineer Rodrigo César Rocha Lacerda (Institute of Aeronautics and Space – IAE), manager of the VLM-1 project, for providing the essential information needed for the development of this work.

Authorship statement. The authors hereby confirm that they are the sole liable persons responsible for the authorship of this work, and that all material that has been herein included as part of the present paper is either the property (and authorship) of the authors, or has the permission of the owners to be included here.

References

[1] Y. Xianglong, J. Zhou, H. Liang, Z. Jiang, and L. Wu, "Mechanical metamaterials associated with stiffness, rigidity and compressibility: a brief review", *Prog. Mater. Sci.*, vol. 94, pp. 114–173, 2018.

[2] B. M. Luccioni, R. D. Ambrosini, and R. F. Danesi, "Analysis of building collapse under blast loads", *Eng. Struct.*, vol. 26, no. 1, pp. 63–71, 2004, doi: 10.1016/j.engstruct.2003.08.011.

[3] A. A. Deleo, J. O'Neil, H. Yasuda, M. Salviato, and J. Yang, "Origami-based deployable structures made of carbon fiber reinforced polymer composites", *Compos. Sci. Technol.*, vol. 191, no. September 2019, p. 108060, 2020, doi: 10.1016/j.compscitech.2020.108060.

[4] C. Lv, D. Krishnaraju, G. Konjevod, H. Yu, and H. Jiang, "Origami based mechanical metamaterials", *Sci. Rep.*, vol. 4, 2014, doi: 10.1038/srep05979.

[5] H. Yasuda, Y. Miyazawa, E. G. Charalampidis, C. Chong, P. G. Kevrekidis, and J. Yang, "Origami-based impact mitigation via rarefaction solitary wave creation", *Sci. Adv.*, vol. 5, no. 5, 2019, doi: 10.1126/sciadv.aau2835.

[6] R. C. R. Lacerda, "VLM-1," *Instituto de Aeronáutica e Espaço*, 2020.

[7] M. Motavalli, C. Czaderski, A. Schumacher, and D. Gsell, "Fibre reinforced polymer composite materials for building and construction", in *Textiles, Polymers and Composites for Buildings*, Elsevier Ltd., 2010, pp. 69–128.

[8] C. O´Connel, "Reusable rockets explained", *Cosmos Magazine*, 2018.